

Remarkable independence of dynamical polarization potentials of the underlying potential

R. S. Mackintosh*

School of Physical Sciences, The Open University, Milton Keynes, MK7 6AA, United Kingdom

N. Keeley†

National Centre for Nuclear Research, ulica Andrzejka Sołtana 7, 05-400 Otwock, Poland



(Received 9 July 2018; published 28 August 2018)

The dynamical polarization potential (DPP) generated by the coupling of specific reaction channels to the elastic channel can be determined by inverting the elastic channel S matrix from a coupled reaction channel (CRC) calculation. The “bare” potential of the CRC calculation is then subtracted from the inverted potential to yield a local representation of the DPP. Here we study the extent to which the DPP calculated in this way depends upon the bare potential. We find that the DPP caused by coupling to pickup channels, for 30.3 MeV protons scattering from ^{40}Ca , turns out to be qualitatively and almost quantitatively unaffected by substantial changes in the bare potential. This puts the properties of DPPs established in this way on a firmer foundation.

DOI: [10.1103/PhysRevC.98.024624](https://doi.org/10.1103/PhysRevC.98.024624)

I. INTRODUCTION

It is known that the elastic scattering of protons on nuclei is strongly influenced by pickup coupling to deuteron channels. The effective contribution of pickup channel coupling to the nucleon optical model potential (OMP) is substantial; see Refs. [1–5] and earlier work cited therein. This contribution cannot be represented by a smooth (Woods-Saxon-like) radial form, and phenomenological fits to precise elastic scattering data with a wide angular range lend support to this. This is arguably important since folding models based on a local density approximation do not appear to support the radial forms implied by reaction channel calculations.

Whether l dependence or nonsmoothness, in the form of a degree of undularity or “waviness,” is the more appropriate representation is debatable since for any l -dependent potential there is always a (nonsmooth) l -independent potential with the same S matrix S_{lj} and therefore the same observables. The inconvenient fact is that representing the effects of coupling to pickup channels with a local and l -independent dynamical polarization potential (DPP) leads to a potential that exhibits some undularity. Such a potential cannot be represented by a uniformly renormalized folding model potential based on a local density model. The coupled reaction channel (CRC) formalism leading to these conclusions is well developed and includes finite range effects and nonorthogonality terms which are incorporated in the widely applied FRESKO code [6].

It might be argued that the undulations in the DPP are spurious and result from the particular choice of “bare” potential. The bare potential refers to the elastic channel potential of the CRC calculation. The DPP is determined by applying $S_{lj} \rightarrow V(r) + \mathbf{I} \cdot \mathbf{s} V_{\text{SO}}(r)$ inversion to the elastic

channel CRC S matrix S_{lj} and subtracting the bare potential from the result. This inversion process itself, properly applied, does not generate spurious waviness, and a secondary result of the present work will support that claim. The primary purpose of the present work is to test an implicit assumption applied in many determinations of DPPs: this assumption is that the DPP determined as described here, i.e., CRC followed by inversion, is not strongly influenced by the choice of bare potential. If that is true, then the undulatory properties of the DPP are clearly not spurious.

In recent work [1], it was found that for protons scattering on ^{16}O , coupling to pickup channels generated an overall attractive DPP. The magnitude of the attraction was substantial and markedly changed the overall radial form of the real potential. This was in marked contrast to what had been found [5] for the case of protons on ^{40}Ca where coupling to the $\frac{3}{2}^+$ ground state of ^{39}Ca (pickup of $\frac{3}{2}^+$ neutron) generated repulsion and the inclusion of $\frac{5}{2}^+$ states increased that repulsion. The radial form for the DPP when the $\frac{5}{2}^+$ states were included was similar to that for the DPP with just the $\frac{3}{2}^+$ ground state coupled. In fact, some of the $\frac{5}{2}^+$ results for ^{40}Ca were found to be wrong due to an error in the version of the CRC code FRESKO that was used. It was subsequently found [7] that including the complete set of pickup states generated a much smaller degree of repulsion than the $\frac{3}{2}^+$ state alone, as quantified by ΔJ_R . Extensive calculations are under way to clarify both the problem with Ref. [5] and other properties of the DPP, including dependence on the charge of the nucleon projectile. These studies strongly motivate the question addressed here: How do the properties of the DPP, as determined by the CRC-plus-inversion method, depend upon the choice of the bare potential? This question is relevant to all studies of this kind.

In all the cases referenced above and in what follows, the pickup contributions are quantified as follows: the elastic

*raymond.mackintosh@open.ac.uk

†nicholas.keeley@ncbj.gov.pl

channel S matrix S_{ij} from the CRC calculation is subject to $S_{ij} \rightarrow V(r) + \mathbf{l} \cdot \mathbf{s} V_{SO}(r)$ inversion and the difference between the resulting potential and the bare potential is identified as a local representation of the DPP caused by the coupling; see Ref. [3] for more details. The formal DPP is both l dependent and nonlocal, see Refs. [8–10] where the nonlocality is distinct from that due to exchange and we refer to it as dynamical nonlocality. Some of the undulatory (wavy) properties of l -independent DPPs can be attributed to the underlying l dependence of the formal DPP.

In the following we study two cases of coupling, each to a state of ^{39}Ca . The two states have very different Q values: one is the $\frac{3}{2}^+$ ground state, Q value -13.41 MeV, the other is a state at 6.5132 MeV representing the weighted contribution of nine $\frac{5}{2}^+$ states. The Q value is -19.92 MeV. The large excitation energy of this state leads to a number of interesting features including a smaller overall magnitude of the DPP.

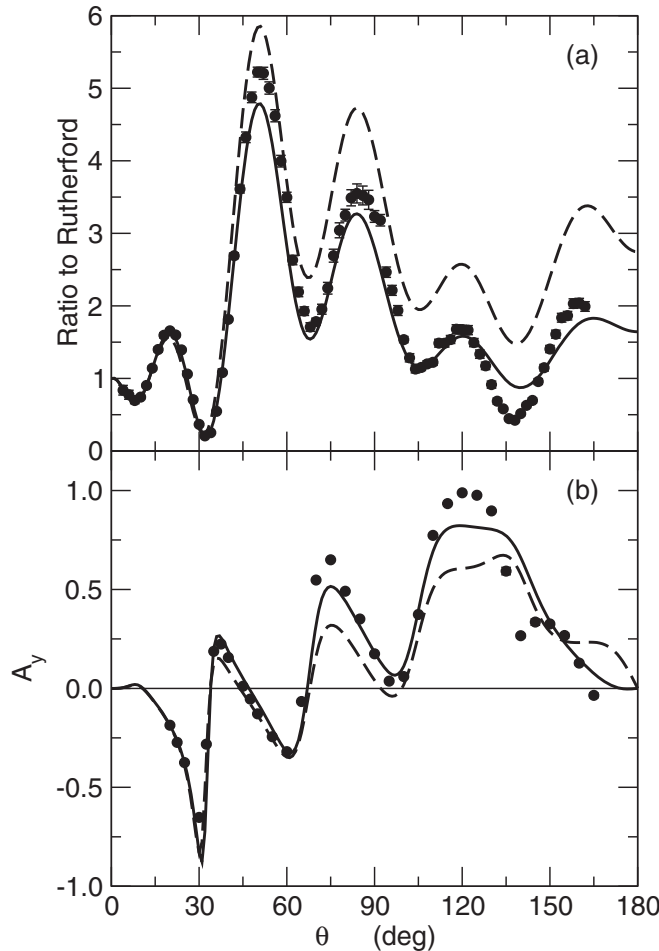


FIG. 1. For 30.3 MeV protons on ^{40}Ca , the solid lines represent the fit to the elastic scattering angular distribution (top panel) and analyzing power (lower panel) when coupling to the $\frac{3}{2}^+$ ground state is included in a search on the conventional Wood-Saxon parameters. The dashed lines present the observables with the coupling switched off. The dots represent the experimental data, Ref. [12] for the DCS and Ref. [13] for the AP.

II. EVALUATING THE DEPENDENCE UPON BARE POTENTIAL

The DPP calculations referred to above were carried out with the bare potential applied in Ref. [5], which we refer to in tables, figures, and text as PRC85. The use of this fixed bare potential enabled the evaluation of dynamic nonlocality for coupling to a range of channels. However, with or without the varied coupling, the fit to the elastic scattering data is far from perfect. Does that matter? It thus becomes natural to ask to what extent the properties of the DPP depend upon the choice of bare potential. In principle it is possible to search on the parameters of the bare potential to fit the elastic scattering differential cross section (DCS) and analyzing power (AP) data for any choice of coupled channels. The resulting DPP can be calculated directly for each bare potential. But to carry out a comprehensive parameter search for the full set of coupled channels, as used in PRC85, is a formidable computing task with the available facilities. Moreover, to determine the DPP for each particular set of coupled channels, the search would have to be repeated with those channels included, and the study of dynamical nonlocality in Ref. [1] would have been impossible since it presupposes a fixed bare potential.

We have chosen to fit elastic scattering DCS and AP data with a search on the parameters of the bare potential for CRC

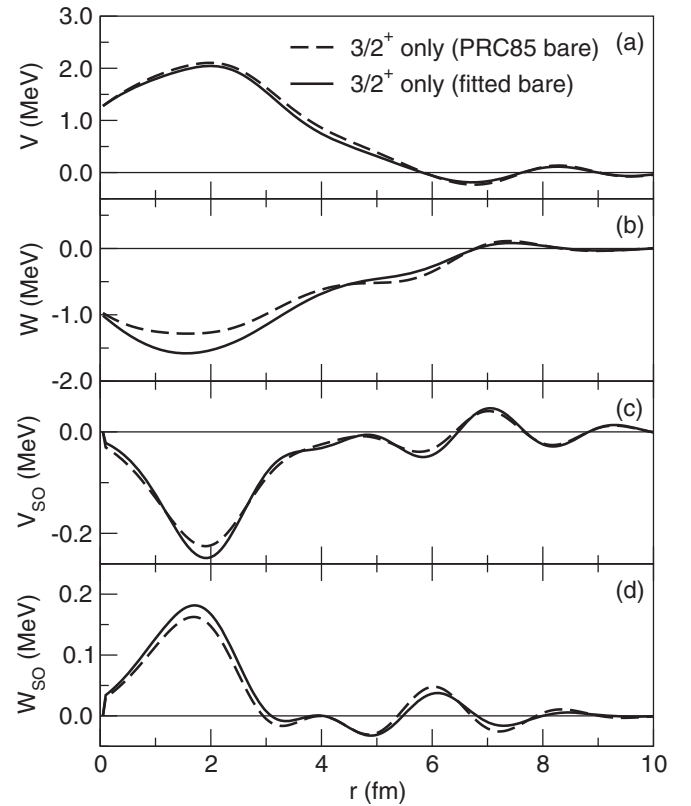


FIG. 2. For 30.3 MeV protons on ^{40}Ca , the solid lines present the DPP caused by coupling to the $\frac{3}{2}^+$ ground state with the bare potential found by fitting the elastic scattering data. The dashed lines present the DPP calculated with the standard (PRC85) bare potential. The panels present, from the top down, the real central, imaginary central, real spin-orbit, and imaginary spin-orbit components.

TABLE I. For 30.3 MeV protons scattering from ^{40}Ca , the properties of the DPP induced by (p, d) coupling. The volume integrals ΔJ of the four components are expressed in MeV fm^3 . The ΔR_{rms} column gives the change in rms radius of the real central component (in fm). $\Delta(\text{Reac CS})$ defined in the text is in mb as is State CS, the reaction cross section to the $\frac{3}{2}^+$ or $\frac{5}{2}^+$ state. R is $\Delta(\text{Reac CS})/\Delta J_R$.

Bare potential	State coupled	ΔJ_R	ΔJ_{IM}	ΔJ_{RSO}	ΔJ_{IMSO}	ΔR_{rms}	$\Delta(\text{Reac CS})$	State CS	R
Fitted	$\frac{3}{2}^+$	-11.79	14.81	0.929	-0.303	0.029	63.63	9.50	4.29
PRC85	$\frac{3}{2}^+$	-12.88	14.57	0.848	-0.291	0.033	51.63	7.93	3.55
Fitted	$\frac{5}{2}^+$	-4.43	17.71	0.958	0.546	0.026	88.55	8.60	5.00
PRC85	$\frac{5}{2}^+$	-4.58	18.18	0.995	0.568	0.030	67.05	7.32	3.69

calculations with coupling to a single pickup state for two different choices of that state. The form of the potential was standard Woods-Saxon, as defined in Ref. [11], including a complex spin-orbit term. For both pickup couplings we have two calculations of the DPP calculated with different bare potentials: (i) the PRC85 bare potential and (ii) the potential found to fit the elastic scattering observables with coupling to the specific reaction channel included.

In the first case, we optimized the parameters of the bare potential to fit the elastic scattering data when there was coupling to the $\frac{3}{2}^+$ ground state of ^{39}Ca . The fit (Fig. 1) is not perfect, but no Woods-Saxon-like potential can fit the data without coupling, so it is not surprising that coupling to just the $\frac{3}{2}^+$ state does not give an exact fit. The elastic channel S matrix S_{lj} from this CRC calculation was inverted and the searched bare potential was subtracted to yield the DPP for

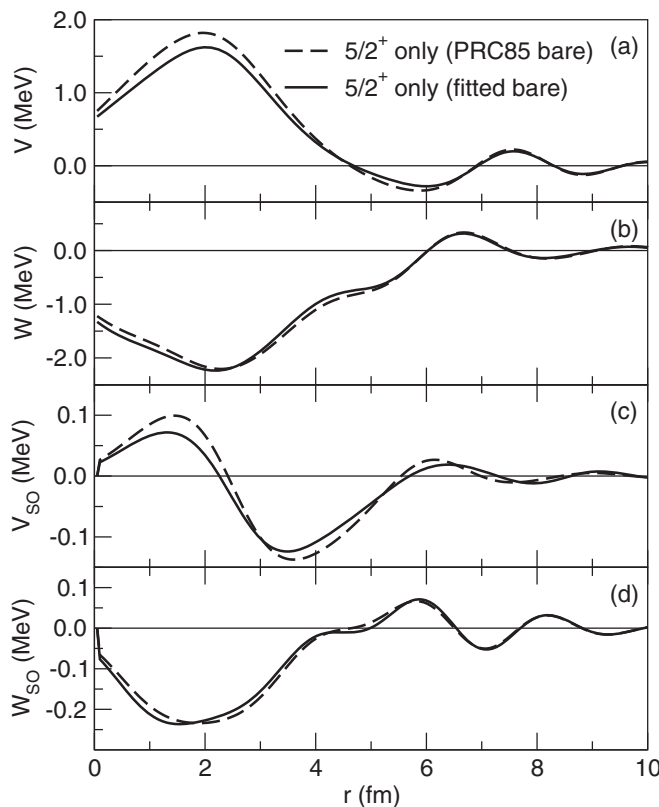


FIG. 3. Same as Fig. 2, but for the DPP caused by coupling to the $\frac{5}{2}^+$ lumped state.

the $\frac{3}{2}^+$ coupling, presented as the solid lines in Fig. 2. The dashed lines represent the DPP for coupling to the same state calculated with the PRC85 bare potential. The first two lines of Table I compare the characteristics of the two DPPs, and it can be seen that all the properties are essentially the same. The largest difference displayed in that table is for $\Delta(\text{Reac CS})$, the increase in reaction cross section when the coupling is turned on. The large differences in $\Delta(\text{Reac CS})$ are simply a consequence of the considerable difference in the bare potential and do not reflect the consistency of the inversion. In fact, the reproduction of the details of the shapes of the smaller terms, shown in Fig. 2, is remarkable and we conclude that the

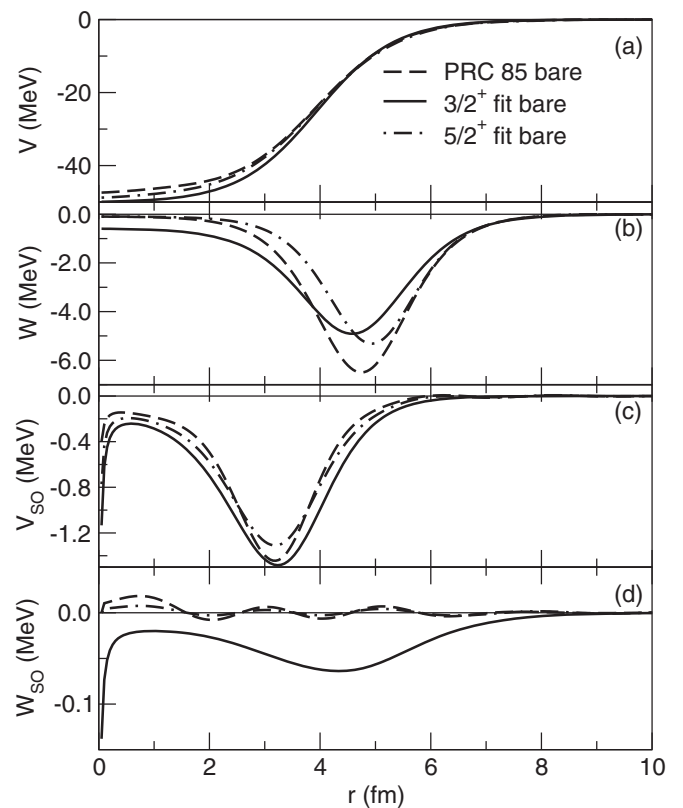


FIG. 4. For 30.3 MeV protons on ^{40}Ca , the three bare potentials: dashes represent the PRC85 bare potential, the solid line is for the case with coupling to the $\frac{3}{2}^+$ ground state, and the dot-dashes represent the bare potential with coupling to the $\frac{5}{2}^+$ state specified in the text. The panels present, from the top down, the real central, imaginary central, real spin-orbit, and imaginary spin-orbit components.

TABLE II. Characteristics of the three bare potentials: the PRC85 and the two fitted potentials. R_{Rrms} and R_{IMrms} are in fm. The final column presents the reaction cross section in mb.

Potential	J_R	R_{Rrms}	J_{IM}	R_{IMrms}	J_{RSO}	J_{IMSO}	REAC CS
PRC85	408.91	4.1144	109.37	5.267	9.329	-0.007	925.77
Fitted $\frac{3}{2}^+$	420.48	4.0248	92.16	5.242	12.359	1.5477	869.88
Fitted $\frac{5}{2}^+$	421.17	4.1550	91.59	5.390	9.903	-0.004	859.10

emissive region around 7 fm in the imaginary central term is not an artefact. The quantity $R = \Delta(\text{Reac CS})/\Delta J_R$ has been informative elsewhere, but variations in quantities related to $\Delta(\text{Reac CS})$ relate to variations in the bare potential and not to the variation or otherwise of the DPP.

The second comparison was carried out for coupling to the state with the large negative Q value, the $\frac{5}{2}^+$ lumped state at 6.5132 MeV. The resulting complex DPP is presented in Fig. 3 with related quantities in Table I.

Including all the states of the PRC85 calculation in a search was not feasible, but calculations involving two states widely separated in energy, and thus in Q value, should give an indication of how independent of bare potential the DPPs are.

The characteristics of the three bare potentials are presented in Table II which includes the rms radii of the real and imaginary central potentials, R_{Rrms} and R_{IMrms} . The last column presents the reaction cross section for elastic scattering (with no coupling) according to these potentials. It will be seen that this is considerably larger for the PRC85 potential in accord with the greater value of J_{IM} , the volume integral of the imaginary central potential. The real central volume integral is significantly less for the PRC85 case. The potentials are plotted in Fig. 4.

III. CONCLUSIONS

From the cases presented here, we may draw the following conclusions:

- (1) The significant quantitative properties of the DPP only depend on the bare potential to a small degree. In this regard ΔJ_R is the difference of two quantities of about 400, one of which is determined by inversion.
- (2) The close similarity in the radial shapes of all four components, derived in both cases with very different bare

potentials, leaves little possibility that the undulatory shape of the DPPs is some sort of artefact.

- (3) In each case the imaginary central term has an emissive region in the surface; this, as well as the general undularity, is typical of local potentials that are S -matrix equivalent (i.e., having the same S_{ij}) to an explicitly l -dependent potential.
- (4) The DPPs of the real and imaginary spin-orbit terms for both cases exhibit undularity that is essentially independent of the bare potential.
- (5) The spin-orbit DPPs are roughly opposite for coupling to the $\frac{3}{2}^+$ and $\frac{5}{2}^+$ states of ^{39}Ca .
- (6) The real central DPP is repulsive toward the nuclear center and attractive near the surface for coupling to both the $\frac{3}{2}^+$ and $\frac{5}{2}^+$ states.
- (7) In both cases the imaginary central DPP is generally absorptive apart from the emissive region in the surface mentioned above.

Note that local regions of emissivity in the surface region of certain potentials do not lead to any breaking of the unitarity limit $|S_{ij}| \leq 1$.

A general conclusion of the present work, as well as the many previous similar DPP calculations, is that the evaluation of folding models by uniform renormalization to get an invariably imperfect (if the data are of high quality) fit is to be deprecated. Much more information would follow if folding models were evaluated by fitting elastic scattering data with model-independent additive terms. If nucleon-nucleus potentials that give precise fits to high-quality elastic scattering data do not have some undulatory character, that fact needs to be established. This work was motivated by investigations, in progress, that seek to understand the surprising results presented in Ref. [7].

[1] N. Keeley and R. S. Mackintosh, *Phys. Rev. C* **97**, 014605 (2018).
 [2] R. S. Mackintosh and N. Keeley, *Phys. Rev. C* **76**, 024601 (2007).
 [3] R. S. Mackintosh and N. Keeley, *Phys. Rev. C* **81**, 034612 (2010).
 [4] N. Keeley and R. S. Mackintosh, *Phys. Rev. C* **83**, 044608 (2011).
 [5] R. S. Mackintosh and N. Keeley, *Phys. Rev. C* **85**, 064603 (2012).
 [6] I. J. Thompson, *Comput. Phys. Rep.* **7**, 167 (1988).
 [7] R. S. Mackintosh and N. Keeley, *Phys. Rev. C* **97**, 069901(E) (2018).

[8] H. Feshbach, *Ann. Phys. (NY)* **5**, 357 (1958); **19**, 287 (1962).
 [9] G. H. Rawitscher, *Nucl. Phys. A* **475**, 519 (1987).
 [10] G. R. Satchler, *Direct Nuclear Reactions* (Clarendon, Oxford, 1983).
 [11] C. M. Perey and F. G. Perey, *At. Data Nucl. Data Tables* **17**, 1 (1976).
 [12] B. W. Ridley and J. F. Turner, *Nucl. Phys.* **58**, 497 (1964).
 [13] V. Hnizdo, O. Karban, J. Lowe, G. W. Greenlees, and W. Makofske, *Phys. Rev. C* **3**, 1560 (1971).